University of Maryland, College Park

Technical Design Report

Advisors

Dr. James Baeder	Aerospace Engineering	baeder@umd.edu
Dr. VT Nagaraj	Aerospace Engineering	vnagaraj@umd.edu

Authors

Andrew Nixon	President, Electrical Lead	Electrical Engineering – Sophomore
Dakota Brakob	Engineering Lead, Structures Lead	Aerospace Engineering – Senior
David Pape	Controls Lead, Aerodynamics Lead	Aerospace Engineering – Senior
Molly Ding	Structures Member	Mechanical Engineering – Junior

May 23, 2021

Contents

1 Executive Summary

The University of Maryland, College Park Wind TERPines team submits this technical document to the Department of Energy Collegiate Wind Competition (CWC) as a detailed description of a small-scale wind turbine, the final configuration of which is a Variable Pitch Horizontal Axis Wind Turbine. The entirety of the competition took place during the pandemic, making construction and testing of a turbine more challenging. In light of these issues, many of the original parameters of the competition have been modified. The team strived to incorporate as much of the design process as possible into a virtual environment. Much of the assembly and testing was done either in small groups or compartmentalized and conducted individually. The team had no access to any on-campus wind tunnels, so the team created a makeshift rooftop mount to test in a parking lot. Johns Hopkins University graciously allowed us to use their wind tunnel two days as well. From these two testing methods, the team was able to collect a sufficient amount of qualitative data to prove our design's effectiveness.

Table 1: Key Design Features of Variable Pitch 3-Bladed Horizontal Axis Wind Turbine

	Significant Features	**Description**
Aerodynamics	Tail Fin	150 mm span, 90 mm chord, Joukowski 9% airfoil. Attached on top and bottom of nacelle for passive yawing.
	Blades	SG6043 blades printed from PLA and attached to pitch collective.
Controls	Hotwire Anemometer	Wind Sensor Rev. C hotwire anemometer. Feedback of flow velocity and temperature to microcontroller.
	Optical Encoder	B83609 optical encoder. Feedback of RPM to microcontroller.
	Pitch Mechanism	Used to collectively pitch blades using mounted servo based on microcontroller feedback.
	Power Sensor	INA260 power sensor. Feedback of power to microcontroller.
Electronics	Voltage Sensor	Common Voltage Sensor. Feedback of voltage under 25 V to microcontroller.
	Generator	Turnigy Gimbal Motor. kV of 31 V/RPM.
Structures	Car Mount	Mount constructed from wooden planks to fix turbine to vehicle. Used for makeshift testing.
	Nacelle	Nacelle constructed from PLA plates and aluminum extrusions.
Performance	Cut-in	Windspeed 3 m/s; Design rotor speed 445 RPM; power approximately 3 W
	Rated	Windspeed 11 m/s; Design rotor Speed 1633 RPM; power 54 W

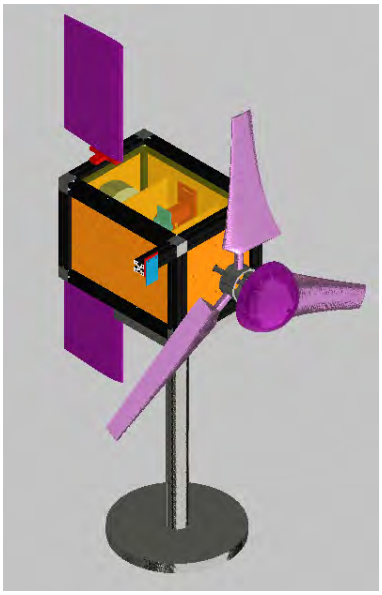

Figure 1: CAD of the wind turbine assembly in Autodesk Inventor 2021

2 Conceptual Design

2.1 Introduction

For the conceptual design process the team utilized an Analytical Hierarchy Process (AHP) followed by a Pugh Matrix evaluation and debates of the optimal design. This section will detail the conceptual design processes previously discussed in our Conceptual Design Report.

2.2 Design Objectives

We designed our turbine with the constraints imposed by the CWC rulebook in mind. There are maximum geometries that limit turbine component dimensions including the rotor and non-rotor parts needing to be contained within a 45x45x45 cm cube. Additionally, the wind turbine will be expected to have cut-in wind speeds between 2.5-5.0 m/s, as well as maintain rated power from 11-13 m/s. Further, to maintain proper safety the turbine should be capable of safely shutting down during two different times at any wind speed, and successfully restart at any wind speed above 5 m/s. Lastly, in compliance with electrical standards, voltage must be DC at the PCC and is always required to be at or below 48 volts.

2.3 Analytical Hierarchy Process

The team held many discussions comparing the relative importance of ten chosen design criteria against one another on a scale of less important (1/9) to more important (9) in varying degrees. Columns were then normalized and the weight of each criterion were averaged to obtain the relative importance of criteria. The AHP matrix is shown in figure 2. Definition of each criterion is provided in table 2.

Table 2: Criteria Definitions

	Weight	Definition
Cut-In Speed	3.6	This is the free stream speed at which the turbine begins to produce usable power. A lower cut-in speed is preferable. This task is worth 25 points.
Power Curve Task	10.0	This is the performance of our turbine in the Power Curve Performance Task, which is worth 50 points. Because this task is weighted towards low speeds, stable power curve performance at these speeds will be preferable.
Yaw Control	1.0	This measures how complex the system to rotate the turbine into the wind is. A less complex system is preferable.
Flow Simplicity	5.5	Measure of how complex the flow the team needs to model around the turbine is. More complex flows are harder to predict and may have unintended consequences. A less complex flow is preferable. Smooth flows reduce vibrations and lead to more stable performance.
Rotor speed Control	7.2	Ability for the rotor to adjust to various wind speeds. Consideration of how complex the rotor speed control system is. A less complex system is preferable.
Ease of Commission	1.1	Measure of how long it will take to commission the turbine at the competition, construction is considered in the other items. A shorter commission time is preferable.
Safety Task	4.1	A completely unsafe turbine will not be allowed to test. In addition to this, the safety task is worth 50 points. This involves restart and shutdown processes. A more efficient emergency response is preferable.
Overall Safety	1.8	How safe to be around it when working
Durability Task	5.4	The Durability task involves yawed flow from 6 to 13 m/s, and is worth 25 points. Performance under rapidly changing conditions is preferable.
Reliability	1.5	Measures how egregious the potential failure modes are. This is separated from the other items to allow the designs to be compared on a more level playing field on those items. Less egregious and fewer failure modes are preferable

2.4 Pugh Matrix

The Pugh Matrix the team used is shown in figure 3. Criteria weights were determined by the AHP previously discussed. Based on extensive discussion, the team evaluated the performance of each concept in each criterion against the baseline. The team chose the Variable Pitch Horizontal Axis

	Cut-In Speed	Power Curve Performance	Yaw Control	Flow Complexity	Rotorspeed Control	Commission Complexity	Safety Task	Durability Task	Reliability	Overall Safety	Total
Cut-In Speed	1.00	0.33	7.00	1.00	0.33	5.00	1.00	0.33	5.00	5.00	26.00
Power Curve Performance	3.00	1.00	9.00	3.00	1.00	7.00	3.00	1.00	7.00	7.00	42.00
Yaw Control	0.14	0.11	1.00	0.14	0.14	1.00	0.14	0.33	0.33	0.33	3.68
Flow Complexity	1.00	0.33	7.00	1.00	1.00	5.00	3.00	1.00	5.00	3.00	27.33
Rotorspeed Control	3.00	1.00	7.00	1.00	1.00	7.00	1.00	1.00	3.00	3.00	28.00
Commission Complexity	0.20	0.14	1.00	0.20	0.14	1.00	0.20	0.14	1.00	1.00	5.03
Safety Task	1.00	0.33	7.00	0.33	1.00	5.00	1.00	3.00	3.00	1.00	22.67
Durability Task	3.00	1.00	3.00	1.00	1.00	7.00	0.33	1.00	3.00	3.00	23.33
Reliability	0.20	0.14	3.00	0.20	0.33	1.00	0.33	0.33	1.00	0.33	6.88
Overall Safety	0.20	0.14	3.00	0.33	0.33	1.00	1.00	0.33	3.00	1.00	10.34
Total	12.74	4.54	48.00	8.21	6.29	40.00	11.01	8.48	31.33	24.67	

Figure 2: Analytical Hierarchy Process Matrix

Wind Turbine (HAWT) as our baseline, as this was last year's design. A + signifies greater, ++ signifies much greater, - signifies lesser, – signifies much lesser, and S signifies equivalent. The team then multiplied each value with the weight, with -2, -1, 0, 1, 2 being the values assigned to –, -, S, +, and ++ respectively. The total score for a configuration is the sum of all the weighted scores for each criterion. A score less than 0 signifies lower performance than the baseline, and a score greater than 0 signifies higher performance than the baseline. The team compared these concepts against one another over many Zoom discussions until a consensus was reached.

Criteria	Weight	VP HAWT	FP HAWT	FP SHAWT	VP SHAWT	FP VAWT	VP VAWT	DB HAWT	DB VAWT
Cut-In Speed	3.6	S	-	-	+	+	++	++	++
Power Curve Task	10.0	S	-	S	+	S	+	--	--
Yaw Control	1.0	S	S	S	S	++	-	S	++
Flow Simplicity	5.5	S	S	-	S	-	-	--	-
Rotorspeed Control	7.2	S	-	-	S	--	--	-	-
Ease of Commision	1.1	S	+	S	-	+	-	-	+
Safety Task	4.1	S	-	-	S	-	-	-	-
Durability Task	5.4	S	-	--	-	+	S	--	-
Overall Safety	1.8	S	S	-	-	S	S	+	+
Reliability	1.5	S	S	--	-	+	+	-	-

					Totals				
Cut-In Speed		0.0	-3.6	-3.6	3.6	3.6	7.2	7.2	7.2
Power Curve Task		0.0	-10.0	0.0	10.0	0.0	10.0	-20.0	-20.0
Yaw Control		0.0	0.0	0.0	0.0	2.0	-1.0	0.0	2.0
Flow Simplicity		0.0	0.0	-5.5	0.0	-5.5	-5.5	-11.0	-5.5
Rotorspeed Control		0.0	-7.2	-7.2	0.0	-14.4	-14.4	-7.2	-7.2
Ease of Commision		0.0	1.1	0.0	-1.1	1.1	-1.1	-1.1	1.1
Safety Task		0.0	-4.1	-4.1	0.0	-4.1	-4.1	-4.1	-4.1
Durability Task		0.0	-5.4	-10.8	-5.4	5.4	0.0	-10.8	-5.4
Overall Safety		0.0	0.0	-1.8	-1.8	0.0	0.0	1.8	1.8
Reliability		0.0	0.0	-3.0	-1.5	1.5	1.5	-1.5	-1.5
Grand Total		0.0	-29.2	-36.0	3.8	-10.4	-7.4	-46.7	-31.6

Figure 3: Pugh Matrix

Using the Pugh Matrix, the team narrowed down the eight concepts to three: the Variable Pitch HAWT, the Variable Pitch Shrouded HAWT, and the Variable Pitch Vertical Axis Wind Turbine (VAWT). Ultimately, the Variable Pitch HAWT was chosen as our design. This was because the control was less complex than for a VAWT, and its superior cut in speed and power curve. The Variable Pitch HAWT additionally had the option of attaching a shroud to once the team finished the baseline design. However, the shroud proved to complex to implement.

3 Preliminary Design

3.1 Introduction

The Variable Pitch HAWT is the conceptual design the team chose. The preliminary design process involved testing of various turbine subsystems before a full prototype of the Variable Pitch HAWT was built and tested. Generators were tested using a dynamometer, the aerodynamics were tested using an exhaust fan, structural integrity was tested using cantilever beams, and blade integrity

was tested using a spin up test to 1700 RPM with a DC power supply. This section will detail the preliminary design processes previously discussed in our Subsystem Testing and Assembly Report.

3.2 Beam Bending

Beam bending tests were conducted to experimentally determine the strength of 3D printed parts with various infill types. 200 mm by 20 mm by 2 mm cantilever beams were printed using 20%, 50%, and 80% infill settings, with each infill setting printed in two different orientations: printed flat with a 200mm by 20mm base and printed on its side with a 200mm by 2mm base. The back end of each beam was clamped to a table with a sharp corner, and the unclamped length L was measured with a ruler. For each beam the area moment of inertia was calculated. After each beam was clamped, a laser diode was taped to its end and projected onto a wall 1.3 m (D) away, as shown in figure 4. A baseline marking was made on the wall and a mass of 11.2 g was hung from the free end. The distance the laser traveled down the wall (H) was then measured with a ruler. This process was repeated for a second added mass (22.3 g total), and the maximum deflection of each beam was calculated as $\delta = HL/D$. Finally, the modulus of elasticity was calculated as $E = PL3/(3\delta I)$. The 20% infill beams printed in a flat orientation had the highest average elastic modulus of 2.907 GPa, and the 80% infill beams printed in a flat orientation had the lowest average elastic modulus of 1.064 GPa.

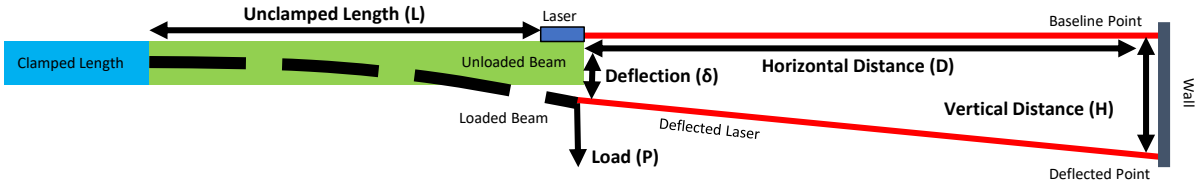

Figure 4: Experimental setup for beam bending tests

3.3 Aerodynamics & Spin Up

The test article the team constructed is shown in figure 5. This design was highly simplified and used to test basic aerodynamic and structural properties of the turbine. The frame was constructed from aluminum MakerBeam extrusions and was mounted on a testing stand. Parts printed from PLA were used to mount two 6 mm bearings. The 6 mm shaft passed through and was constrained by electrical tape. The blades were mounted to the shaft using the pitch collective the team had decided on. A gear was placed on the shaft between the two bearings and meshed with a gear attached to a DC motor which was mounted to the extrusions with another PLA part. This design was placed downstream of an exhaust fan. The blades were able to cut in effectively under this flow. The second test was intended to test blade failure at high rpm. The DC motor was powered with a DC power supply of up to 32 V. No failure occurred up to 2000 RPM (highest power able to be supplied), well past our design RPM.

4 Detailed Design

4.1 Introduction

A front view photograph of the wind turbine in a feathered pitch setting is shown in figure 6a. A front view photograph of the wind turbine in an unfeathered pitch setting is shown in figure 6b, less the blades. A dimensioned view of the wind turbine is shown in figure 7. This section will describe how all the components of our turbine were assembled together. Details on design of specific components or subsystems is discussed in later sections. Throughout this section, figure 9 will be used, with components referenced parenthetically. 3D printed parts are orange, red, or purple, while metal parts are grey or black. Sensors are blue.

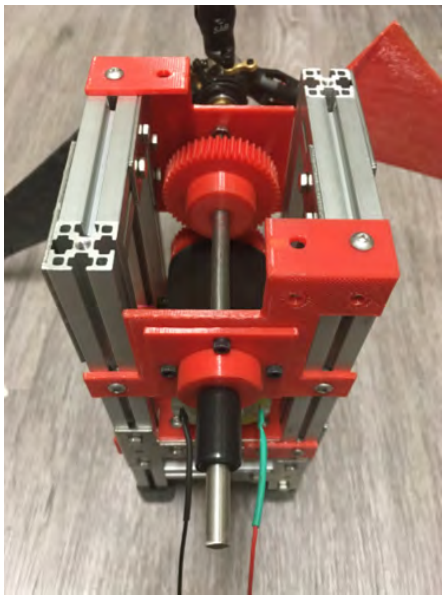

Figure 5: Test article used to determine cut in speed performance and blade integrity

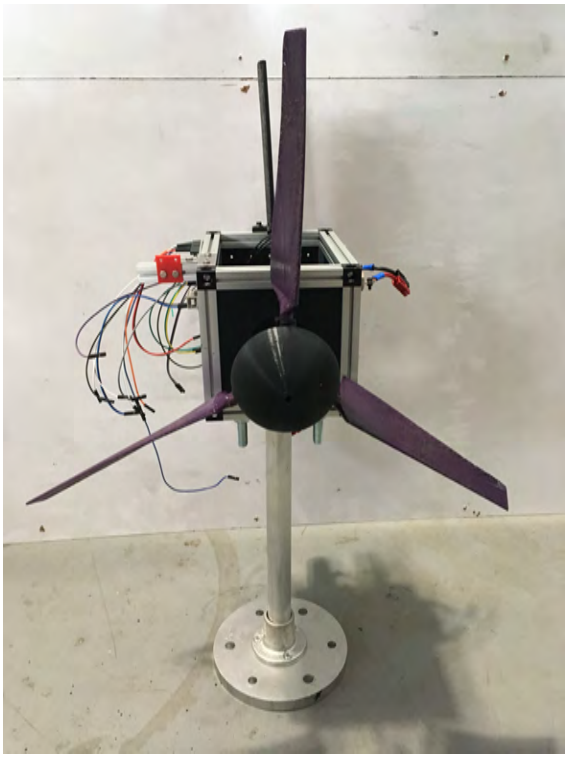

(a) Front view of feathered wind turbine

(b) Front view of unfeathered wind turbine

Figure 6: Feathered and unfeathered blades

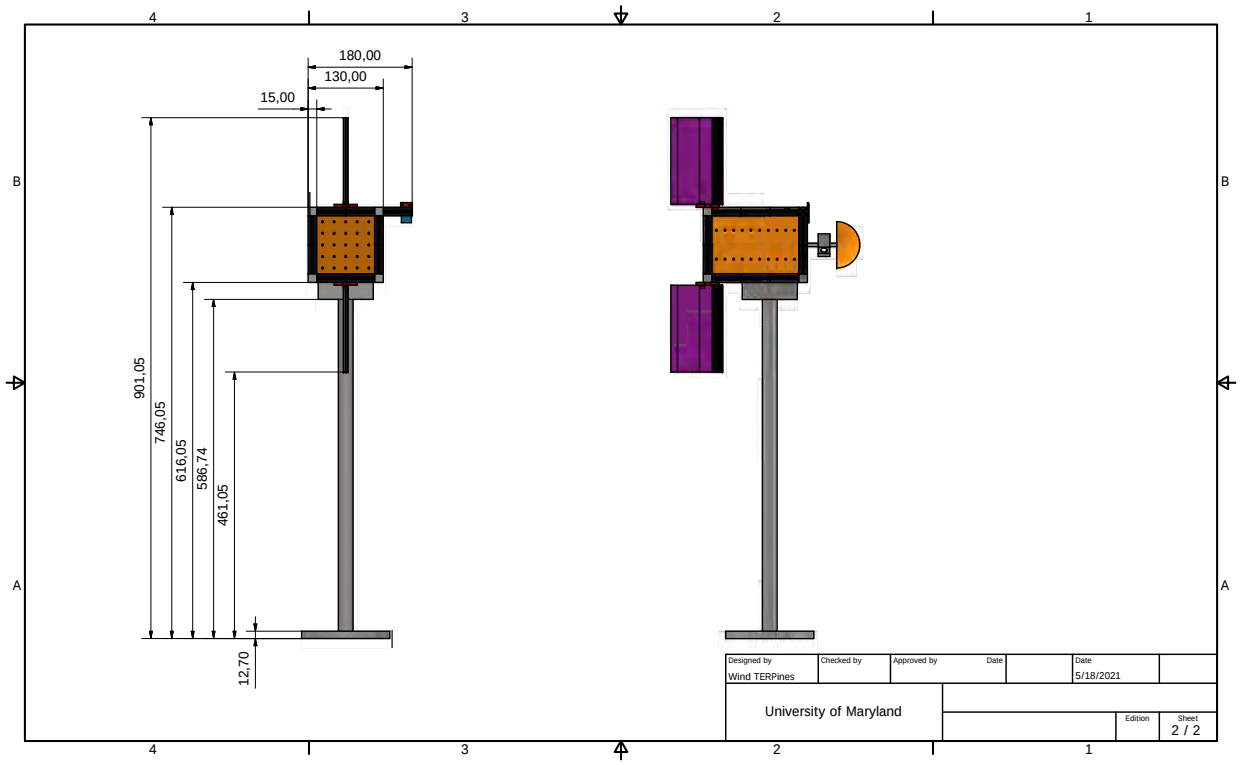

Figure 7: Dimensioned view of wind turbine

4.2 Tower Assembly

The tower (1) for this year's design was the same as last year's. The tower was constructed from an aluminum tube with 1 in outer diameter and $\frac{3}{4}$ in inner diameter. The pipe was fixed with a set screw to an aluminum flange, which was built according to specs from the CWC rulebook. The aluminum tube passed through a set of block bearings (2), shown in figure 8. These bearings require fairly low torque to spin for their size, have a self-aligning feature, and two set screws which were used to secure it to the tower. The bearings have four M10 mounting holes which were used to attach the tower to the nacelle.

4.3 Rotor Assembly

The team 3D printed two sets of three blades (one for backup) for the wind turbine. These three blades (3, not shown) were mounted to a pitch collective mechanism (4), which changes blade pitch depending on linear displacement of the collective along the shaft (5). The collective mechanism was allowed to slide along the shaft, which the blades remained in a fixed position about 25 mm from the shaft end. The rotor hub (6), which was a hemisphere of 80 mm diameter was fixed to the protruding shaft.

Figure 8: PGN UCF205-16 bearings with 1 in diameter [7]

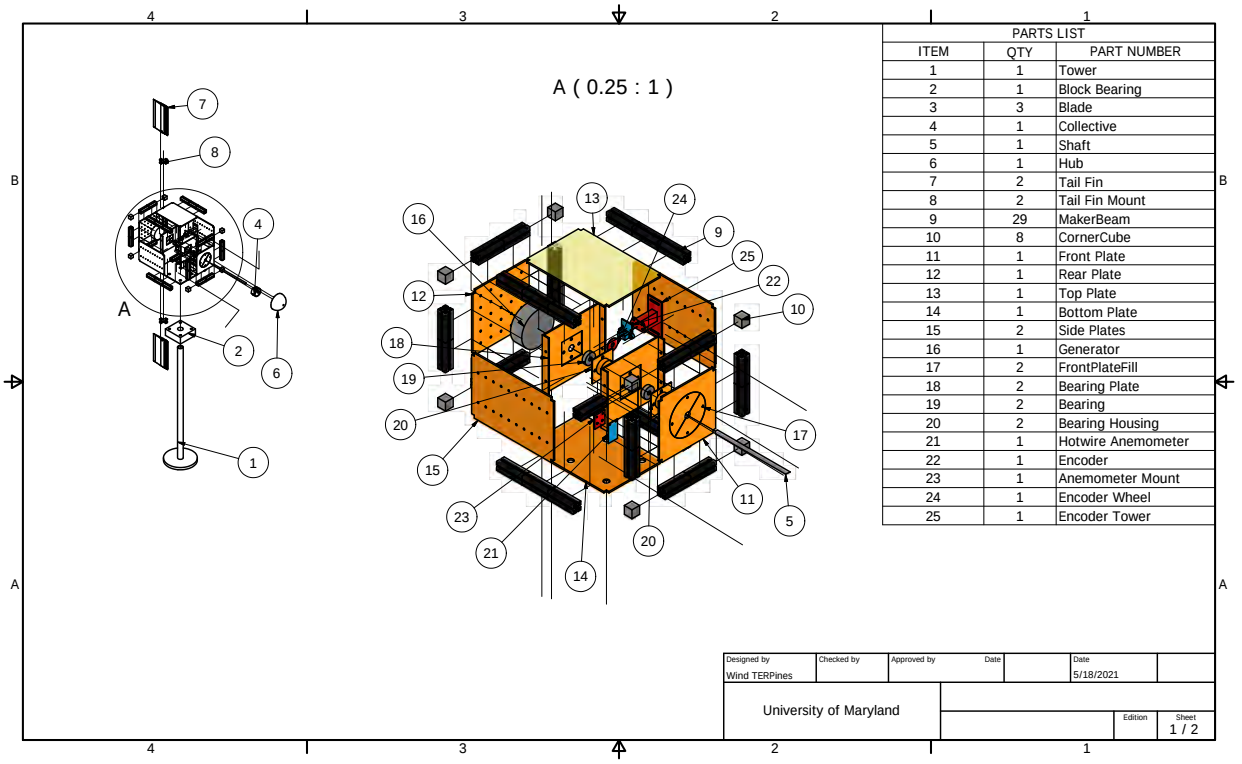

Figure 9: Exploded view of wind turbine assembly

4.4 Tail Fin Assembly

To yaw the turbine, the team used a passive system comprised of two 150 mm vertical tail fins (7). These two tail fins attach to two plus shaped mounts (8) with two slots and two holes. The slots were used to attach the tail fin. Then the holes were used to secure the tail fin and mount to the MakerBeam extrusion. Both tail fins were attached in the center of the back top and bottom extrusions. This system will be discussed further in section 5.1

4.5 Nacelle Assembly

Each MakerBeam extrusion (9) has a 15 mm by 15 mm cross section, and beams used were either 100 mm or 150 mm long. Along each side of an extrusion is a groove for M3 nuts. In the center of the cross section is a threaded M3 hole, which the team used to form the 8 nacelle corners using MakerBeam corner cubes (10). The nacelle cross section from a frontal view is 130 mm by 130 mm, and is 180 mm by 180 mm from a side view. A front plate (11), a back plate (12), a top plate (13), a bottom plate (14), and two side plates (15) were 3D printed from PLA to slide into the grooves of the extrusions and give the nacelle a defined surface. The generator (16) was attached to the back plate through four threaded M3 mounting holes on the back of the generator. The top plate has no features and is just a solid plate, but is transparent in CAD to show interior detail. The bottom plate has four M10 holes for mounting the bearing, as well as a $\frac{3}{4}$ in hole for feeding wiring from the nacelle through the tower. The front plate has two fill pieces (17) which are attached once everything has been assembled.

4.6 Retained Design Properties

Only three significant design properties were retained from 2020 – the generator, the passive nature of the yaw system and the collective pitch. Figure 10 shows the generator that was used in 2020, however the selection process was unique to this year. The passive nature of the yaw system was retained for its simplicity, and the drag-based grid fin from the 2020 design was replaced with a lifting vertical fin this year. The collective was again retained for simplicity; however, it is also likely that the team would have arrived at the same, or similar, choice of collective had the decision been made to redesign the system.

Figure 10: Retained selection of motor[6]

4.7 Shaft Alignment

The shaft was aligned through three constraints. First, the shaft was connected to the generator through an adapter piece which was screwed onto the generator via threaded mounting holes on the front of the generator. This alone would be insufficient for alignment of the shaft, so two bearing plates (18) were printed from PLA. These bearing plates have two holes on each end for fixing to the nacelle. Along the side plates, there are twenty 3 mm holes in a 2 by 10 grid spaced equally. The bearing plates are fixed to the left and right side plates through an M3 screw, and the multitude of holes on the side plates allows for an adaptable placement of the bearing plates. In the center of the bearing plates there are four M3 holes. The bearings (19) are placed in the center of the plate. A bearing housing part (20) is then placed over the bearings and fixed to the bearing plate using M3 screws.

4.8 Sensor Assembly

The two position dependent sensors in the CAD model are the hotwire anemometer (21) and the encoder (22). The hotwire anemometer needs to be facing the flow, and a bit downstream of the rotor so there is minimal interference. The hotwire anemometer came with two mounting holes, but both were M2 and could not mount to the extrusions. A small anemometer mount (23) was printed from PLA with two M2 holes to mount the anemometer to, and two M3 holes to mount to the extrusion. To minimize flow interference, a 50 mm extrusion was placed along the 150 mm extrusion. Its position could be adjusted by loosening the brackets connecting the 50 mm extrusion and sliding it downstream or upstream. The position shown in the CAD was not the final position the team chose, which was about halfway along the 150 mm beam instead of at the front end. Plans were in place to calibrate the anemometer beyond manufacturer specification should slipstream interference require such action. The encoder operates using a lasergate and optical encoder disc (24). The issue was that the sensor needs to be very close to the shaft so that it can register the encoder. The team accomplished this by 3D printing a tower (25) for the encoder which mounts to the side plates using slotted M3 holes. At the top of the tower are holes precisely located for mounting the sensor to, and the tower was about 40 mm tall.

5 Aerodynamics

5.1 Tail Fin Design

The tail fin for the turbine this year differs from past years in its design being lifting. The yawing method is still passive however. For simplicity of comparison, Q-Blade (described in section 5.2) was utilized to more easily and more readily compare the airfoils against each other in lift v alpha and drag v alpha. From this plot the Joukovsky 9% airfoil was selected for its steep lift curve with a low lift slope within 3 degrees of aligned with the flow, as shown in figure 11[1].

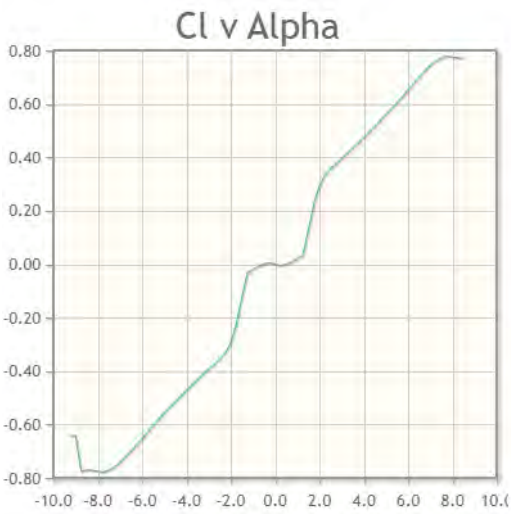

Figure 11: C_L v. Alpha for Joukovsky 9% airfoil

This low lift slope near 0 degrees alpha gives a damping effect to the passive yaw system, while the steep lift slope outside that range allows the turbine to yaw into the flow quickly if disturbed. For simplicity of manufacture, the tail fin itself was designed with a rectangular planform of span 150mm and chord 90mm. The fin would then be made twice to attach above and below the turbine. As the yaw system was tested, the design of the fin and mount would allow for the tail fin to be moved rearward on extra MakerBeams to increase the yawing moment arm. This configuration decision was made because of the low lift forces on the fin as shown in figure 20.

5.2 Rotor Blade Design

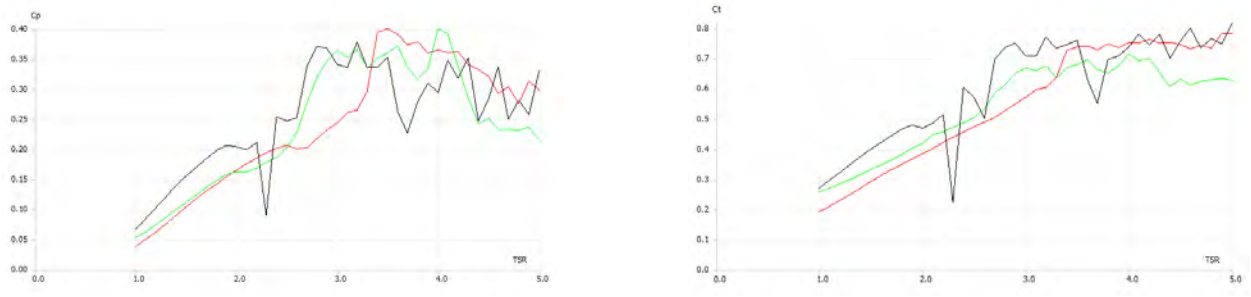

(a) C_p v. TSR

(b) C_t v. TSR

Figure 12: C_P and C_t plots. For both plots, the 2020 baseline design is in red, the SG6043 is in black, and SG6042 in green

Blade design was done using Q-Blade[8], an open source blade element momentum (BEM) theory turbine blade design suite. The suite is capable of optimizing twist angle and chord based on a variety of criteria. These blades were designed using lift/drag twist optimization and Betz rd optimization settings. Learning from past years' research and design work the SG series airfoils were chosen because of their performance at low Reynolds numbers. From here, a series of 6 blades were designed. 3 blades that were compound blades of the SG6040 airfoil (which is designed as a root foil[2], and one of the 3 other foils, and 3 blades of a single airfoil 6041-6043[3][4][5]. These blades were compared to each other using Q-Blades BEM plots, such as those shown in figure 12.

Although the curves in figure 12 are not smooth curves, they do agree with an in house BEM analysis done using MATLAB. Table 4 in Appendix A defines blade foil, chord and twist at several stations along the length of the blade.

Based on the plots of power coefficient v tip speed ratio, the decision was made that the SG6043 blades were the best option for the turbine. This is due to the SG6043 blades having a shallower more stable power coefficient curve, while being comparable to the other blades in many other major metrics. The compound blades performed approximately equally to those with only one airfoil. Due to this fact, and the geometry of the compound blades making them both less structurally sound and more difficult to manufacture, the single airfoil blade was selected.

From here, Q-Blade's built in stress analysis and vibrational analysis tools. Using a provided density and Young's modulus for the blades, and the loading from turbine simulations, Q-Blade can show a heat map of blade stresses, as shown in figure 13. With the stress mapping indicating a maximum stress of 4.53 MPa, yielding a safety factor of 7.9 for the ultimate stress of prototype material PLA at 35.9 MPa; and the lowest natural frequency of 408 Hz being significantly above design rotor speed of 36 Hz, the blade design was considered final and prototyped as shown before in figure 6.

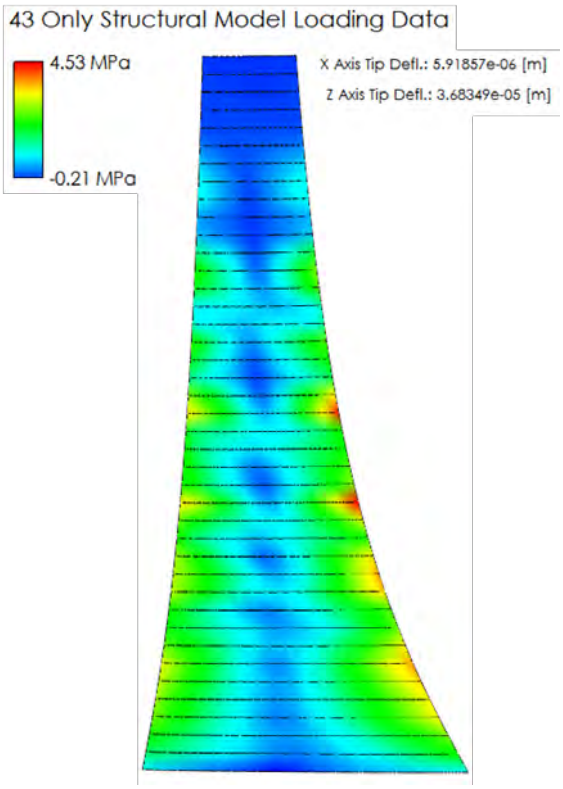

Figure 13: Heat map of blade stresses

A power curve plot generated by Q-Blade is shown in figure 14. From design, and experimentally confirmed, at the cut in speed of 3 m/s the turbine generates approximately 2.7 W. This increases toward an ideal rated power of 60 W at a wind speed of 11 m/s. Furthermore, the turbine is expected to generate 15 W at the heaviest weighted wind speed of 7 m/s in ideal conditions with no losses. Mechanical and electrical losses are anticipated to reduce output by approximately 5-10% yielding an expected rated power of 54 W at 11 m/s and 1650 RPM.

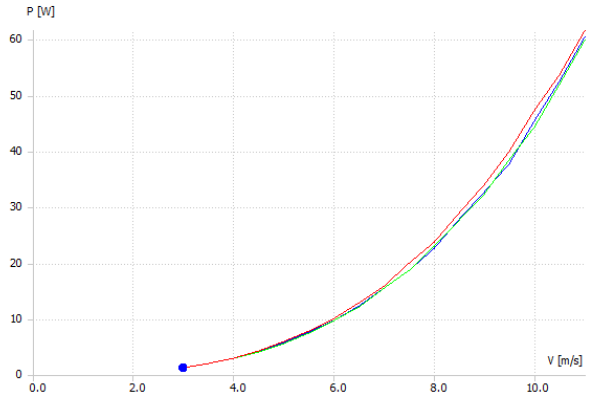

Figure 14: Power v Flow Velocity; TSRs 2.75, 3.0, and 3.25 in blue, green and red curves respectively

6 Electronics

6.1 Generator Selection

The generator selected for this design is a Turnigy Gimbal 5208 with a reported Kv of 31. This is the same generator that was used in last year's design, because its low Kv is desirable for this competition. An equivalent number of revolutions per minute with this motor will result in a higher output voltage than a generator featuring a higher Kv could. Also, at a rated speed of 1700 RPM, this generator will output 54 volts, which is only slightly higher than the maximum allowable load voltage of 48 volts. Therefore, minimal downward scaling will be needed. It was not necessary to modify the generator in any way. It features mounting threads on the front and back which were used to position it inline with the rotor shaft.

6.2 Power Rectification

A common full wave rectifier was used to convert the three phase alternating input to a single phase output. This was done using diodes rated for 10 amperes of current, which should remove all concern about exceeding any limits of flow. The final design featured Anderson Powerpole connectors on the inputs and outputs so that this component could become modular. If troubleshooting was needed, it could easily be removed without the worry of damaging other circuits that may have been soldered in place.

6.3 Power Regulation

The selected generator is capable of reaching voltage potentials that could exceed the maximum allowable 48 volts. During a test, it was observed that the raw potentials coming from the rectifier reached nearly 60 volts, so clearly a modification was needed. The team's buck/boost converters have a maximum allowed input of 36 volts, so again some sort of a solution is needed. A 2-to-1 voltage divider which divides the input by half would remove all concern for exceeding the 36 volt threshold.

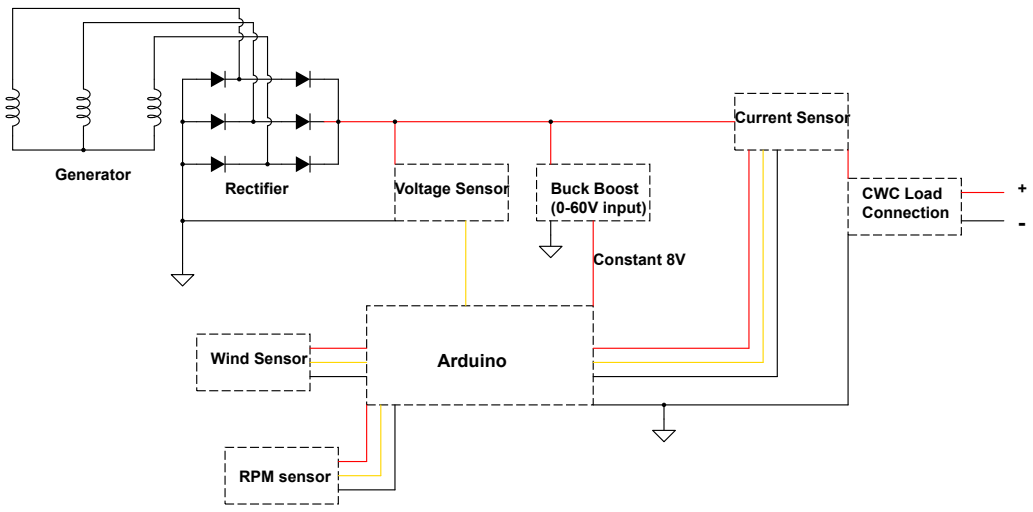

Figure 15: Line diagram schematic for the turbine

7 Turbine Control

7.1 Introduction

The turbine is designed to be controlled by a variable pitch rotor, similar to the way a constant speed propeller works. As the rotor reaches rated speed, the microcontroller would send a signal to the servo controlling the pitch to step toward feathered. If the rotor is under rated speed, the microcontroller would send a signal to step the pitch away from feathered. The desired rotor speed is set by a switch statement off of a variable containing the wind speed from an anemometer on-board the turbine. This switch statement sets the rotor speed for design tip speed ratio of 3.25. This section details all the components necessary to achieve this blade pitching process, as well as the two operational modes; Rated Speed and Shutdown.

7.2 Actuators

The only active actuation on the turbine is a servo used to pitch the rotor blades. Blade pitching is achieved through a system (similar to a slider-crank mechanism) that converts the rotational motion of a servo motor into linear motion of a pitch collective. The actuation of the servo arm will pull or push a linkage arm that is then connected to the pitch collective, which will allow the blades to turn to different angles. The servo is attached to a side plate of the nacelle by a 3D printed mount with slotted holes for easy adjustment.

7.3 Sensors

The turbine uses a combination of sensors, shown in figure 16, to determine its state. Flow temperature and wind speed are determined using a combined thermistor and hot wire anemometer from Modern Device. This allows the turbine to set the speed which the rotor needs to operate at. Rotor speed is read using an optical encoder B83609 from SongHe which is backed up with a voltage sensor from HiLetGo across the AC/DC rectifier. In order for the microcontroller to change the pitch of the blades, these two sensors have to agree on whether the rotor is above design speed or under design speed. The last set of sensors used to control the turbine comprise the shutdown system. There is of course the required emergency stop button which is used to send an immediate feather signal to the rotor servo. The load disconnect is determined by current in through the load leads dropping to zero, using an Adafruit INA260 voltage/current/power sensor board.

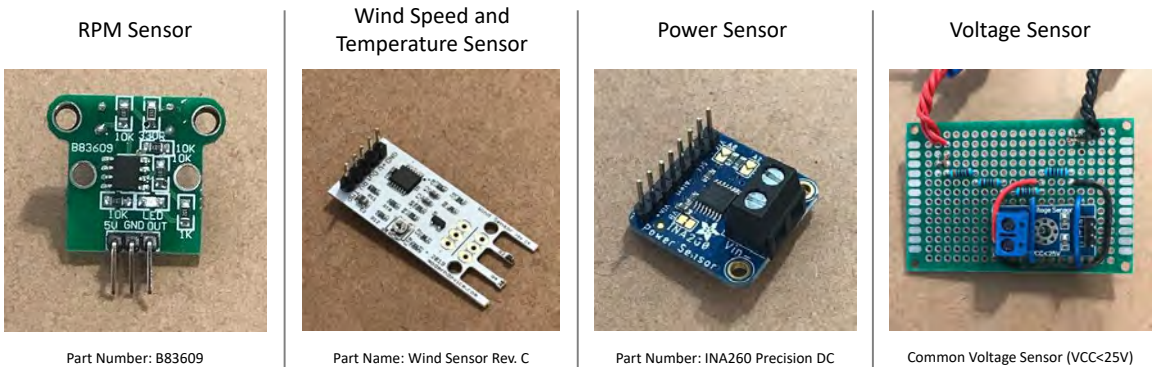

Figure 16: Turbine Sensors

7.4 Microcontrollers

The turbine is centered around an Arduino Uno microcontroller, with the ability to move to an Arduino Mega should further development require the extra pins. The Arduino provides sufficient clock speed to read rotor speed off a 20 slot encoder wheel, while retaining the ability to operate on 5 volts. The other microcontroller considered for the turbine was the Teensy 4.0, which was ultimately disfavored for requiring placement in a breadboard and a power supply of 3.3 volts.

7.5 Control States

The state machine diagram in figure 17 shows the operational states the turbine can be in, as well as the transitions between them. Once commissioned in the wind tunnel, the turbine will remain in an operating state, either startup, rated speed, or shutdown operation. These states are described in more detail in sections 7.6 and 7.7.

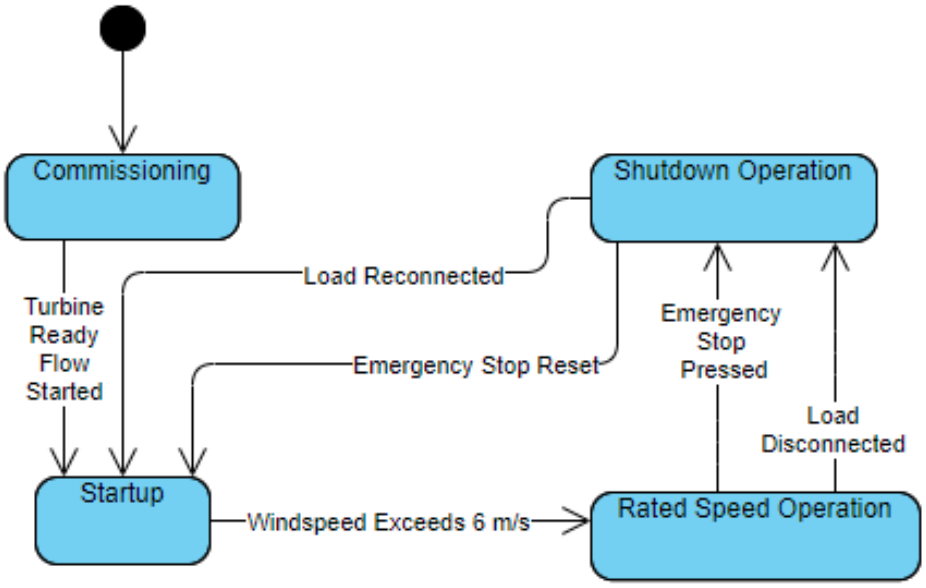

Figure 17: Turbine State Machine Diagram

7.6 Rated Speed Control

When operating at a design speed, the microcontroller will compare the rotor speed from the encoder and the voltage on the voltage sensor with the speed for design tip speed ratio at a given wind speed. From there, provided no override flags are true, the microcontroller will either advance the pitch toward the high RPM state, or reduce it toward feathered. There are two override flags that can be flipped true based on operational conditions. The feather flag overrides speed input and forces the blades into a feathered state. The high RPM flag overrides the speed inputs to set the blade pitch to the highest RPM state. Logic in the code dictates that these two flags cannot simultaneously be true, however the feather flag will take precedence over the high RPM flag in the event this logic fails.

7.7 Shutdown

When shutting down the turbine, the feather flag goes true. When this happens, the microcontroller will set the blade pitch to an adjustable feathered state. This feathered state can be configured to completely feather the blades and stop the turbine completely, or to pitch to a low RPM state that meets the 10% maximum rotor speed definition. If the former is selected, the turbine must be manually restarted. If the latter is selected, the turbine will have sufficient power generation to restart itself.

8 Turbine Testing

The checklist in table 3 shows the commissioning steps in the wind tunnel for the competition. Testing on the car rig described later requires modification to this checklist to accommodate the idiosyncrasies of the rig.

.

Table 3: Commission Checklist

1. Electrical connections	Verify
2. Set screw security	Verify
3. Freedom of rotation	Verify
4. Turbine Tower	Attach to wind tunnel base plate
5. Pitch	Manually set high RPM (Repeated for manual restarts)
6. Common coupling	Connect and verify

The wind tunnel traditionally available to the team was not available since the beginning of COVID-19, so it was necessary to figure out another way of verifying designs.

(a) Side-view of a Toyota Rav4 outfitted with the testing-rig made of 2x4's, ratchet straps, and a lot of screws

(b) A smart phone positioned just behind the turbine was able to capture footage of what was happening while driving

Figure 18: An unorthodox approach to turbine testing

Figure 18 shows the final setup that made it possible for the turbine to experience incoming wind speeds in the range of 0 to 11 m/s. This was done in an empty parking lot at the University

of Maryland. The driver was exclusively focused on driving at all times and a second person was responsible for monitoring the turbine and incoming data. The campus police were also notified each day testing was done so as to avoid any unnecessary altercations. During the car-mounted testing, the team measured qualitatively that when the blades were feathered there was no rotation, and when they were feathered there was rotation. From this, the team concluded that mechanical braking is unnecessary, and that aerodynamic braking was sufficient for the safety task of the competition. The team measured yaw control in the Johns Hopkins University wind tunnel. Even when perturbed to extreme angles greater than 90 degrees, the turbine corrects itself towards the flow in a few seconds. From this the team concluded that yaw control of the turbine was effective.

9 Additional Efforts

Data acquisition is extremely important for this competition. Arduino, or a similar microcontroller, is most often the tool of choice for interpreting incoming analog signals from sensors and converting them to some value that is readable on the serial line or serial monitor of the Arduino Graphical User Interface (GUI). While this system has worked in the past and is indeed good enough in most cases, it could easily be improved. It should be possible to customize the number of plots shown, so that data from any number of sensors can be viewed simultaneously. This is possible with Arduino's serial plotter, but there should be more options for customization. Arduino also doesn't natively export comma separated data to a .dat or a .csv file, which could be problematic and could result in the loss of data. LabVIEW is a very robust program that could quite easily solve all of these problems, but the data acquisition hardware is expensive and the software only recognizes National Instruments brand devices. Not to mention that this hardware is often bulky and would not fit inside the nacelle. Therefore, space exists for a new solution. Python is the language of choice for accomplishing this task because it has a large user-base, is open source and therefore free, and has a package called TKinter that allows users to make custom GUIs.

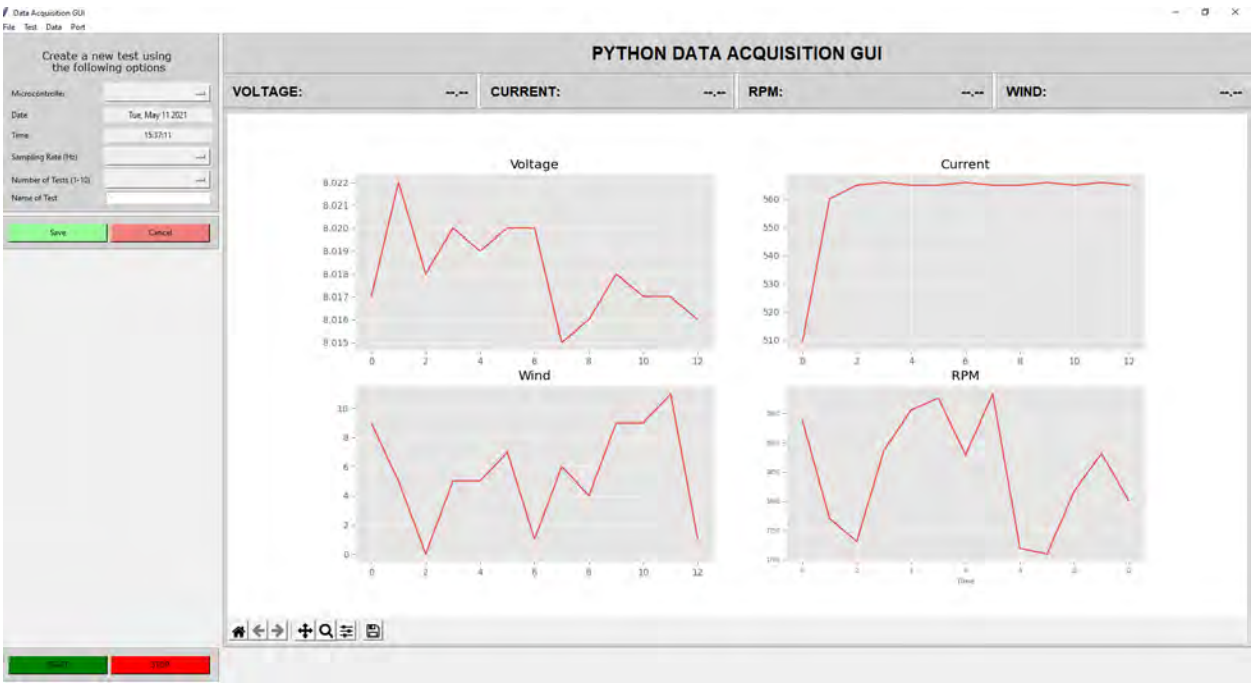

Figure 19: Graphical User Interface for Data Acquisition

Figure 19 shows one possible layout. This was written and compiled from scratch using Python, and every aspect is customizable. The user is first prompted to enter certain information about the test, such as the microcontroller being used, the sampling rate, the number of plots that should be displayed, and a unique name for the test that will be used to generate the .dat file once the test ends. After pressing "Save", and then pressing "START", the program first attempts to connect to the USB port that leads to the microcontroller. Assuming the microcontroller is plugged in and already sending csv data to the serial line, it will read that data at a frequency of the user's choice. If four plots are chosen, as in this figure, then the data is sent in real-time to its corresponding plot. The plots will show the most recent 60 seconds of data, meaning that the plot will appear to slide to the left as time goes on, and each current data point is displayed at the top for quick reference. Once the test is over, the user will click "STOP", and all data is automatically sent to a .dat file with a name specified by the user. The .dat file also contains header information with the date, time, test length, and all column descriptions. This application is obviously not perfect, but it could be improved with time. Another notable advantage is that this is an application that can be run from the command line, and therefore does not require an internet connection in any way. If the team were to do car-mounted testing somewhere off-campus and WiFi was not available, this application would not be affected whatsoever. It has not yet been converted to a single downloadable application, but the team hopes to do this in the future. Then multiple members could each have versions of it on their own systems, taking away the pressure for one single person to have it. It may even be possible to make this project open source to all CWC teams, so that other people would be able to have a free, reliable, and somewhat elegant solution to data acquisition for their turbines that is fully compatible with Arduino. Please contact Dr. Baeder or Dr. Nagaraj (the University of Maryland PI's) if there is interest in this.

10 Conclusions

The team had to make many changes to adapt to the restrictions imposed by the pandemic. The team utilized Zoom meetings and designed many components of the turbine in a distributed manner by assigning those components to members who had the necessary knowledge and equipment to design and build them. For example, Andrew had the vehicle and equipment necessary to build the car mount for the turbine. Dakota had a 3D printer, and handled the CAD and printing of parts. David had the knowledge of QBlade, and handled all the design for the blades and tail fin to be printed. By handling design in a distributed fashion, the team was able to work on multiple design aspects simultaneously, assigned to those equipped best to handle that aspect. The team was not able to collect much quantitative data but collected qualitative data through recordings of the car mount and wind tunnel testing. Through this data, the team was able to demonstrate effectiveness of various design aspects. Passive yaw was effective and efficient, sensor accuracy was calibrated and verified against expected values, the blades cut in at about 3 m/s, and feathering the blades effectively acted as aerodynamic braking.

11 Appendix A: Aerodynamics

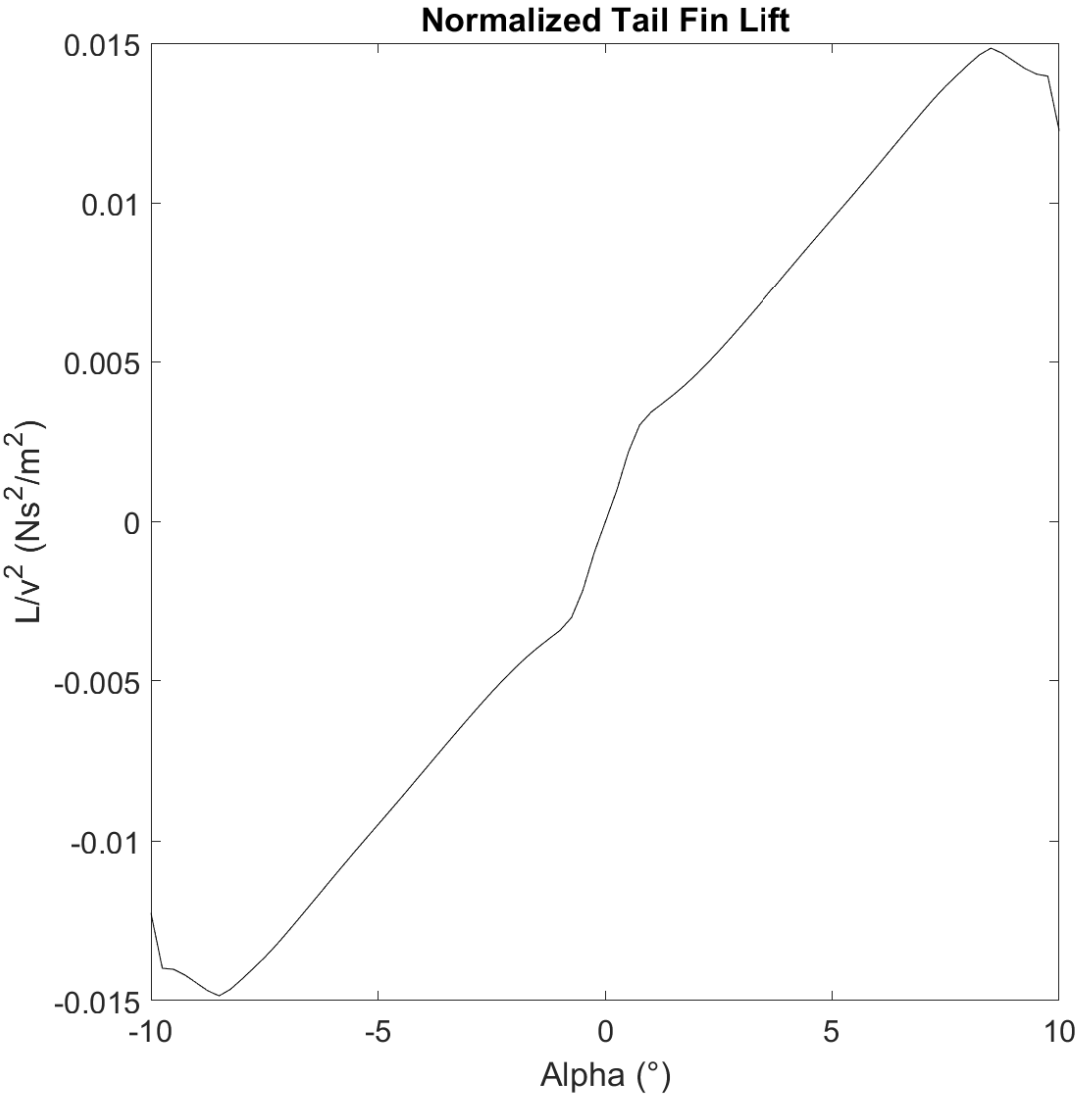

Figure 20: Normalized lift versus angle of attack for Joukowski 9% airfoil with 90 mm chord and 300 mm span

Table 4: Blade specification including mounting point

Radial Position (mm)	Chord Length (mm)	Twist (deg)	Airfoil Name
0.00	10.00	N/A	Circular Foil
5.00	10.00	N/A	Circular Foil
10.00	10.00	N/A	Circular Foil
15.00	10.00	N/A	Circular Foil
20.00	10.00	N/A	Circular Foil
30.00	70.00	20.32	SG6043
35.00	67.38	19.03	SG6043
40.00	64.69	17.85	SG6043
45.00	62.18	16.75	SG6043
50.00	59.84	15.74	SG6043
55.00	57.65	14.80	SG6043
60.00	55.61	13.93	SG6043
65.00	53.69	13.11	SG6043
70.00	51.89	12.35	SG6043
75.00	50.20	11.65	SG6043
80.00	48.61	10.98	SG6043
85.00	47.11	10.36	SG6043
90.00	45.70	9.77	SG6043
95.00	44.36	9.22	SG6043
100.00	43.10	8.70	SG6043
105.00	41.90	8.21	SG6043
110.00	40.77	7.74	SG6043
115.00	39.69	7.30	SG6043
120.00	38.67	6.88	SG6043
125.00	37.69	6.49	SG6043
130.00	36.76	6.11	SG6043
135.00	35.88	5.75	SG6043
140.00	35.04	5.41	SG6043
145.00	34.23	5.08	SG6043
150.00	33.46	4.77	SG6043
155.00	32.72	4.47	SG6043
160.00	32.01	4.19	SG6043
165.00	31.33	3.91	SG6043
170.00	30.68	3.65	SG6043
175.00	30.06	3.40	SG6043
180.00	29.46	3.16	SG6043
185.00	28.88	2.93	SG6043
190.00	28.32	2.70	SG6043
195.00	27.79	2.49	SG6043
200.00	27.27	2.28	SG6043

References

[1] Airfoil Tools. Joukowsky 9% Airfoil, 2021. [Online; accessed April 24, 2021].

[2] Airfoil Tools. SG6040 Airfoil, 2021. [Online; accessed February 27, 2021].

[3] Airfoil Tools. SG6041 Airfoil, 2021. [Online; accessed February 27, 2021].

[4] Airfoil Tools. SG6042 Airfoil, 2021. [Online; accessed February 27, 2021].

[5] Airfoil Tools. SG6043 Airfoil, 2021. [Online; accessed February 27, 2021].

[6] HobbyKing. Turnigy HD 5208 Brushless Gimbal Motor (BLDC), 2021. [Online; accessed May 23, 2021].

[7] PGN Bearings. PGN - UCF205-16 Pillow Block Square Flange Mounted Bearing 1" Bore, 2021. [Online; accessed May 23, 2021].

[8] Technical University of Berlin. QBlade, n.d. [Software; accessed February 5, 2021].